

Innate Immune Cell–Related Pathology in the Thalamus Signals a Risk for Disability Progression in Multiple Sclerosis

Olavi Misin, MD, Markus Matilainen, PhD, Marjo Nylund, MSc, Eveliina Honkonen, MSc, Eero Rissanen, MD, PhD, Marcus Sucksdorff, MD, and Laura Airas, MD, PhD

Correspondence

Dr. Airas
laura.airas@utu.fi

Neurol Neuroimmunol Neuroinflamm 2022;9:e1182. doi:10.1212/NXI.0000000000001182

Abstract

Background and Objectives

Our aim was to investigate whether 18-kDa translocator protein (TSPO) radioligand binding in gray matter (GM) predicts later disability progression in multiple sclerosis (MS).

Methods

In this prospective imaging study, innate immune cells were investigated in the MS patient brain using PET imaging. The distribution volume ratio (DVR) of the TSPO-binding radioligand [¹¹C]PK11195 was determined in 5 GM regions: thalamus, caudate, putamen, pallidum, and cortical GM. Volumetric brain MRI parameters were obtained for comparison. The Expanded Disability Status Scale (EDSS) score was assessed at baseline and after follow-up of 3.0 ± 0.3 (mean ± SD) years. Disability progression was defined as an EDSS score increase of 1.0 point or 0.5 point if the baseline EDSS score was ≥6.0. A forward-type stepwise logistic regression model was constructed to compare multiple imaging and clinical variables in their ability to predict later disability progression.

Results

The cohort consisted of 66 patients with MS and 18 healthy controls. Patients with later disability progression (n = 17) had more advanced atrophy in the thalamus, caudate, and putamen at baseline compared with patients with no subsequent worsening. TSPO binding was significantly higher in the thalamus among the patients with later worsening. The thalamic DVR was the only measured imaging variable that remained a significant predictor of disability progression in the regression model. The final model predicted disability progression with 52.9% sensitivity and 93.9% specificity with an area under the curve value of 0.82 (receiver operating characteristic curve).

Discussion

Increased TSPO radioligand binding in the thalamus has potential in predicting short-term disability progression in MS and seems to be more sensitive for this than GM atrophy measures.

From the Turku PET Centre (O.M., M.M., M.N., E.H., E.R., M.S., L.A.), Turku University Hospital and University of Turku, Finland; Neurocenter (O.M., M.N., E.H., E.R., M.S., L.A.), Turku University Hospital, Finland; Department of Clinical Neurosciences (O.M., M.N., M.S., L.A.), University of Turku, Finland; and Faculty of Science and Engineering (M.M.), Åbo Akademi University, Turku, Finland.

Go to [Neurology.org/NN](https://www.neurology.org/NN) for full disclosures. Funding information is provided at the end of the article.

The Article Processing Charge was funded by the authors.

This is an open access article distributed under the terms of the Creative Commons Attribution-NonCommercial-NoDerivatives License 4.0 (CC BY-NC-ND), which permits downloading and sharing the work provided it is properly cited. The work cannot be changed in any way or used commercially without permission from the journal.

Glossary

ARR = annualized relapse rate; **AUC** = area under the curve; **BIC** = Bayesian Information Criterion; **DVR** = distribution volume ratio; **EDSS** = Expanded Disability Status Scale; **GM** = gray matter; **MS** = multiple sclerosis; **NAWM** = normal-appearing WM; **PF** = parenchymal fraction; **ROI** = region of interest; **RRMS** = relapsing-remitting MS; **SPMS** = secondary progressive MS; **TSPO** = translocator protein; **WM** = white matter.

Gray matter (GM) atrophy is increasingly recognized as a potential imaging biomarker for disease progression in multiple sclerosis (MS).^{1,2} GM atrophy has been shown to associate more closely with clinical disability than conventional white matter (WM) radiologic measures and to predict MS disease progression.³⁻⁷ However, GM atrophy, as we understand it today, represents a late-stage phenomenon of MS pathology, being a consequence of irreversible axonal loss and neuronal death.⁸ Hence, even if usable for prediction of later disability accrual, therapeutic alternatives are limited to affect this outcome. Other *in vivo*-measurable elements of MS disease pathology, such as innate immune cell-related pathology within the GM, may serve as an earlier indicator of progression-promoting pathology and potentially a therapeutically modifiable target.

[¹¹C]PK11195 is a first-generation translocator protein (TSPO)-binding radioligand, which presents increased binding to microglial cells and macrophages in various pathologic settings.^{9,10} TSPO-PET-measurable innate immune cell-related pathology is increased in the normal-appearing WM (NAWM) areas of the MS brain compared with healthy controls.^{11,12} Increased TSPO-PET signal in the NAWM associates with more severe disease^{13,14} and predicts disability progression.¹⁵ TSPO-PET can likewise be used to elucidate the inflammatory component of GM pathology that is invisible to conventional MRI,¹⁶ and patients with MS have been shown to exhibit elevated TSPO-PET signal in GM regions with concomitant more severe disability and cognitive impairment.^{17,18} In this study, we addressed the value of GM TSPO-PET in predicting clinical disability progression in MS and demonstrate that thalamic neuroinflammation predicts short-term disease worsening.

Methods

Participants

Sixty-six patients with MS and 18 age-matched healthy controls were included in the final evaluation. The patients were selected from all patients with MS ($n = 97$) who have undergone TSPO-PET imaging in the Turku PET Centre between 2009 and 2017, whose follow-up duration was between 2.5 and 5.0 years, and who had an EDSS score evaluation within this follow-up time period. 47 patients had relapsing-remitting MS (RRMS), and 19 patients had secondary progressive MS (SPMS). The patients were recruited from the outpatient clinic of the Division of Clinical Neurosciences at the University Hospital of Turku, Finland, and all patients with TSPO-PET imaging and suitable follow-up time were included.

Disability was evaluated with the Expanded Disability Status Scale (EDSS) score. The EDSS scores were determined at baseline and after a follow-up period of 2.5–5.0 years (3.0 ± 0.3 , mean \pm SD). Information on relapses and medication during the follow-up was recorded. Confirmed disability progression was defined as an EDSS score increase of 1.0 point (or 0.5 point if the baseline EDSS score was ≥ 6.0) that was sustained over a 6-month period. The annualized relapse rate (ARR) was determined for the entire disease history from the diagnosis to the time of PET imaging and for the follow-up period. To eliminate the effect of acute focal inflammatory activity on TSPO imaging results or EDSS score, patients were excluded if they had had a clinical relapse and/or corticosteroid treatment within 30 days of imaging or of reevaluation of the EDSS score. Other exclusion criteria were gadolinium contrast enhancement in the baseline MRI, active neurologic or autoimmune disease other than MS, another significant comorbidity, inability to tolerate PET or MRI, and current or desired pregnancy.

MRI Acquisition and Analysis

MRI was performed at baseline. The majority of the MRIs (56 patients with MS and 10 healthy controls) were acquired with a 3T Ingenuity TF PET/MR scanner (Philips). The following sequences were used: axial T2, 3D fluid attenuated inversion recovery (FLAIR), 3D T1, and 3D T1 with gadolinium enhancement. For a subset of 10 patients with MS and 8 healthy controls, a 1.5-T Nova Dual scanner (Philips) was used. Here, the sequences were axial T1, axial T2, coronal FLAIR, and axial 3D-T1 with gadolinium enhancement.

Lesion Segmentation Tool (statistical-modelling.de/1st.html, a toolbox running in SPM8)¹⁹ was used for semiautomated T2 lesion segmentation, and the resulting mask was then manually corrected. T1 lesion mask was manually edited from the finalized T2 lesion mask, and T1 and T2 lesion volumes were obtained from these masks as described previously.²⁰ T1 images with lesion filling were used for autosegmentation of GM regions of interest (ROI) with FreeSurfer 6.0.0 software (surfer.nmr.mgh.harvard.edu/). Five ROIs were chosen for this study: cerebral cortex, thalamus, caudate, putamen, and pallidum. Their volumes were analyzed as parenchymal fractions (PFs), which were calculated for each ROI by dividing the ROI volume by the total intracranial volume. Intracranial volume was calculated in FreeSurfer as a sum of WM, GM, and CSF.

PET Acquisition and Analysis

PET imaging was performed at baseline. The radiochemical synthesis of [¹¹C]PK11195 and imaging with this radioligand were performed as described previously.¹¹ PET was

Table 1 Demographic Information and Clinical Variables of the Study Population

Variable	HC	MS	RRMS	SPMS	RRMS vs SPMS ^a	Progression	No progression	Progression vs no progression ^a
n	18	66	47	19		17	49	
Females, n (%)	13	51 (77)	39 (83)	12 (63)	0.11	12 (71)	39 (80)	0.5
Age, y	42.9 (11.4)	45.2 (9.9)	42.8 (9.1)	51.1 (9.6)	0.006	47.8 (6.9)	44.3 (10.7)	0.3
Disease duration, y	N/A	12.4 (7.4)	10.5 (6.8)	17.1 (6.9)	0.001	15.6 (6.0)	11.3 (7.6)	0.017
EDSS score at baseline (median, IQR)	N/A	3.0 (2.0–3.9)	2.5 (2.0–3.0)	6.0 (3.8–6.5)	<0.001	5.0 (3.5–6.5)	2.5 (2.0–3.5)	<0.001
Follow-up duration, y	N/A	3.0 (0.3)	3.0 (0.3)	3.1 (0.5)	0.7	3.1 (0.3)	3.0 (0.3)	0.5
ARR before baseline (median, IQR)	N/A	0.36 (0.23–0.56)	0.41 (0.24–0.58)	0.30 (0.21–0.46)	0.2	0.41 (0.24–0.47)	0.35 (0.22–0.59)	0.8
Patients with relapses during follow-up, n (%)	N/A	19 (29)	11 (23)	8 (42)	0.15	7 (41)	12 (24)	0.2
Treatment at baseline or ≤2 mo before								
No DMT	N/A	23	11	12	<0.001	9	14	0.2
Moderate-efficacy DMT^b	N/A	35	32	3		7	28	
High-efficacy DMT^c	N/A	8	4	4		1	7	
Treatment within 3 y of MS onset								
No DMT	N/A	21	10	11	0.013	8	13	0.3
Moderate-efficacy DMT^b	N/A	40	33	7		8	32	
High-efficacy DMT^c	N/A	5	4	1		1	4	

Abbreviations: ARR = annualized relapse rate; DMT = disease-modifying treatment; EDSS = Expanded Disability Status Scale; HC = healthy control; IQR = interquartile range; N/A = not applicable; RRMS = relapsing-remitting multiple sclerosis; SPMS = secondary progressive multiple sclerosis.

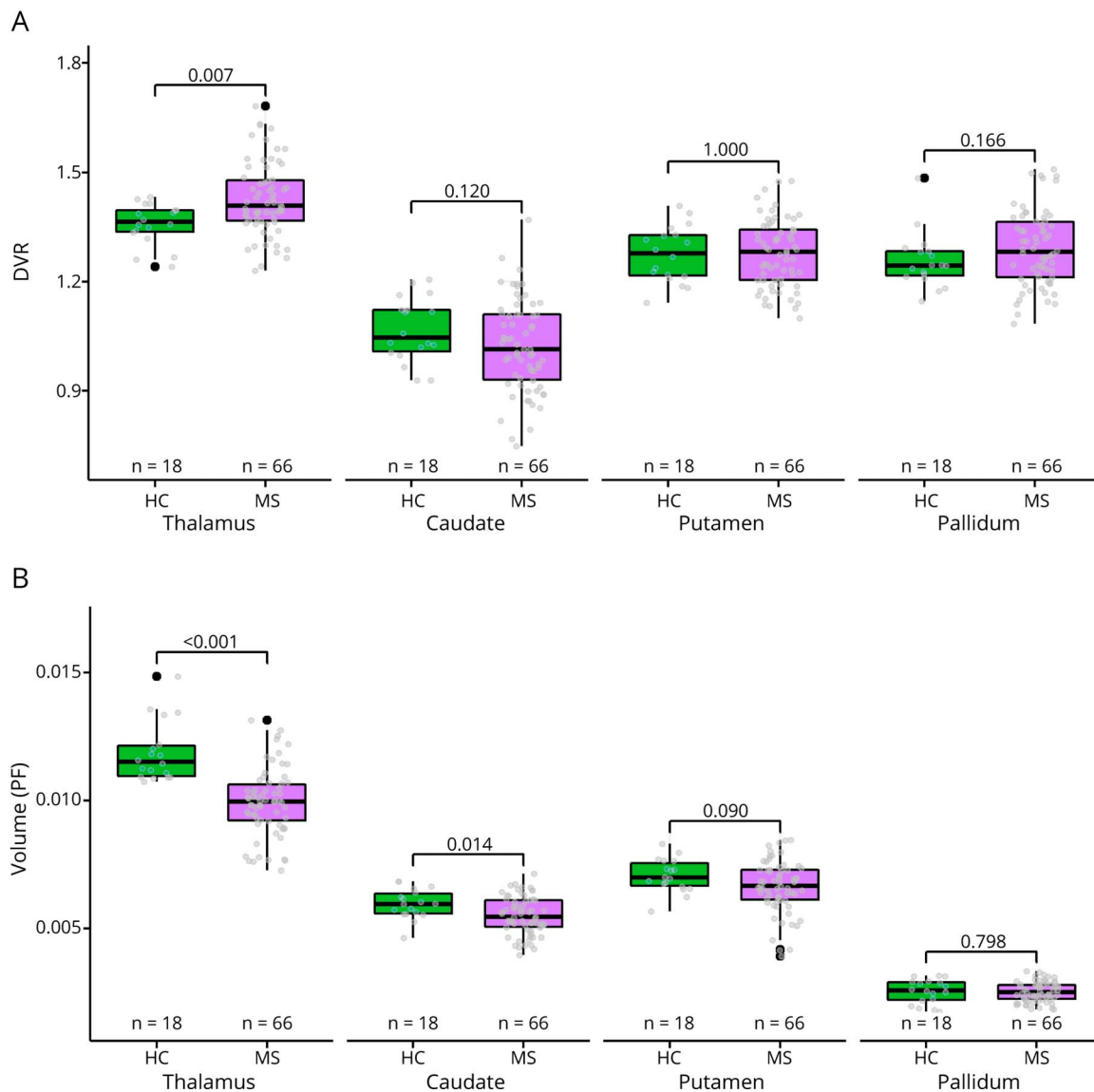
Variables presented as mean (±SD) unless stated otherwise. The Wilcoxon test was used to compare the distributions of continuous variables, and the Fisher exact test was used to compare the distributions of categorical variables.

^a p Value.

^b Interferon beta, dimethyl fumarate, glatiramer acetate, teriflunomide, and fingolimod.

^c Cladribine, natalizumab, ocrelizumab, and rituximab.

Figure 1 Baseline TSPO-PET DVR and MRI Volumes in Patients With MS and Healthy Controls



(A) Patients with MS had a higher DVR in the thalamus compared to healthy controls. (B) Patients with MS had a lower PF of the thalamus and caudate compared to healthy controls. The Wilcoxon rank-sum test was used. DVR = distribution volume ratio; HC = healthy control; MS = multiple sclerosis; PF = parenchymal fraction.

performed with a brain-dedicated ECAT High-Resolution Research Tomograph scanner (CTI/Siemens) with an intrinsic spatial resolution of approximately 2.5 mm. The mean injected dose was 475.0 ± 50.8 MBq (mean \pm SD) for the MS patient group and 489.8 ± 16.4 MBq for the healthy control group.

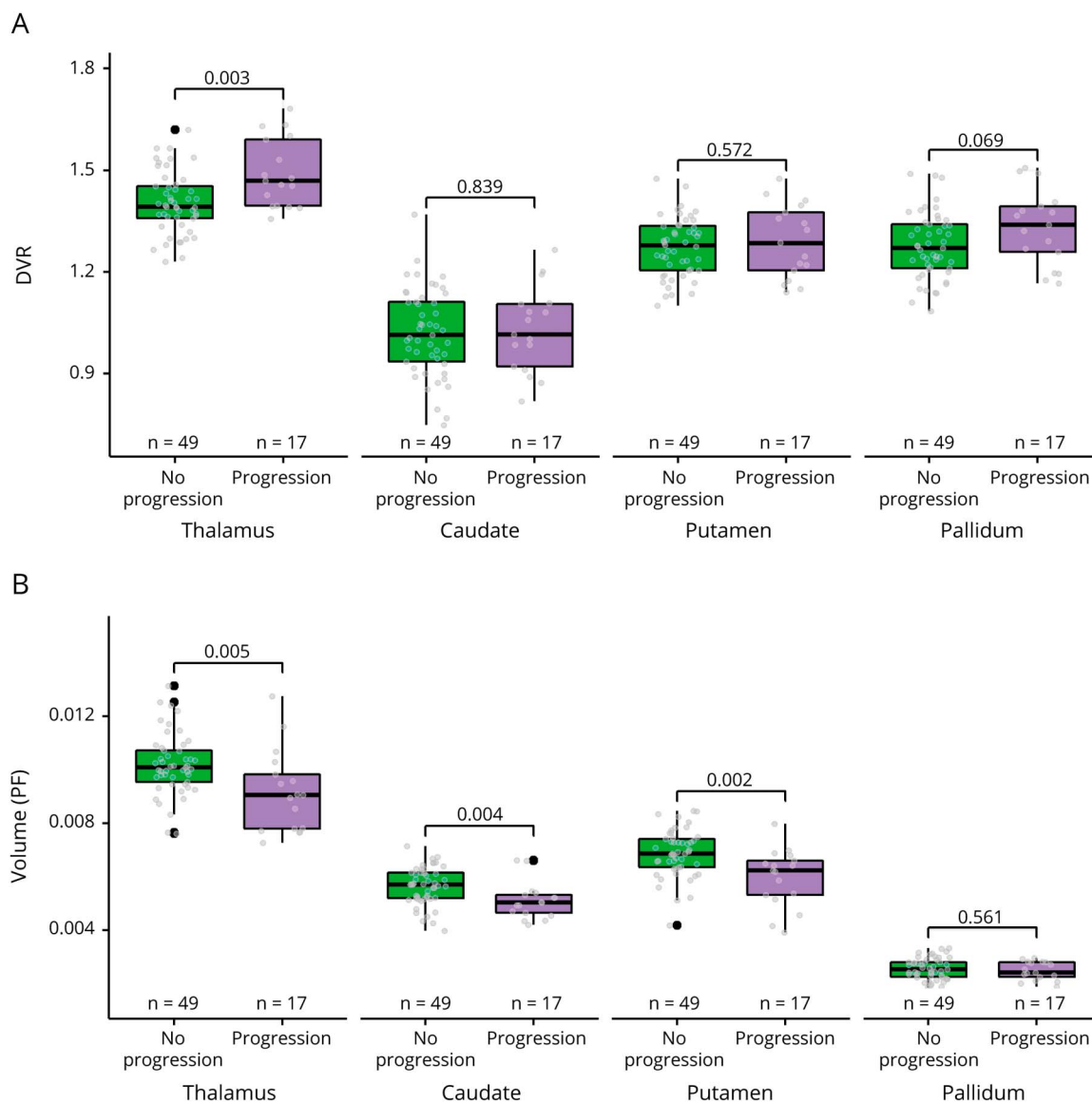
PET images were reconstructed using 17 time frames as described previously.¹¹ The dynamic data were smoothed using a Gaussian 2.5 mm postreconstruction filter. Partial volume correction was performed as described previously using the Geometric Transfer Matrix method with PETPVE12 toolbox in SPM12.¹⁵ Innate immune cell-related pathology was evaluated as specific binding of [¹¹C]PK11195 using the distribution volume ratio (DVR) in prespecified ROIs. The DVR measurements were determined by comparing the time-

activity curves of the ROIs to the reference regions using a supervised cluster algorithm with 4 kinetic tissue classes (SuperPK software, SVCA4 classification).^{21,22}

Statistical Analysis

The statistical analyses were performed using R (version 4.1.1). The Wilcoxon rank-sum test was used to assess differences between subgroups such as patients with MS and controls. Spearman correlation was used to assess relationships between continuous variables. A forward-type stepwise logistic regression model was constructed to determine the best variables predicting disability progression. The main imaging variables used in the modeling were the DVR values and PFs of each ROI and the global T2 lesion volume. Other variables considered were EDSS score at baseline, sex, age,

Figure 2 Baseline TSPO-PET DVR and MRI Volumes in Relation to Disability Progression



(A) Patients with EDSS progression at follow-up had a higher DVR in the thalamus at baseline compared to patients with no EDSS progression. (B) Patients with EDSS progression at follow-up had a lower PF of the thalamus, caudate, and putamen at baseline compared to patients with no EDSS progression. The Wilcoxon rank-sum test was used. EDSS = Expanded Disability Status Scale; HC = healthy control; PF = parenchymal fraction.

disease duration at baseline, duration of the follow-up, ARR preceding baseline, ARR during the follow-up, class of the disease modifying treatment (DMT) at baseline or at most 2 months before, and class of the DMT within the first 3 years after MS onset. All DMTs were categorized into 3 classes: (1) no DMT; (2) moderate efficacy DMTs (interferons, glatiramer acetate, dimethyl fumarate, fingolimod, and teriflunomide); and (3) high-efficacy DMTs (natalizumab, alemtuzumab, ocrelizumab and rituximab).²³

The model building began with a model without any variables, and in each step, the most suitable of the aforementioned variables according to the Bayesian Information Criterion (BIC) was added to the model. This was continued until no

additional variable improved the model. After the final model with the lowest BIC value was established, the model was checked for its assumptions (e.g., multicollinearity and influential values). ORs for progression risk were obtained from the parameter estimates. For continuous variables with smaller ranges, the ORs for a 0.1-unit increase are calculated instead of ORs for a 1-unit increase.

The final model was further validated using a leave-one-out cross validation, in which the probability of disability progression for each observation was predicted using all other observations. Sensitivity and specificity were calculated using contingency tables. For this, if the probability of disability progression based on the model was above 50%, the

Table 2 Association Between Imaging and Clinical Variables and Confirmed Later Disability Progression

Predictors in the final model	Stepwise logistic regression	
	OR	p Value
EDSS score at baseline	2.22	<0.001
Thalamic DVR at baseline	2.28 ^a	0.024

Abbreviations: DVR = distribution volume ratio; EDSS = Expanded Disability Status Scale.

The EDSS score was modeled using forward-type stepwise logistic regression. Model building began with no variables in the model, and the addition of each variable was tested using the Bayesian Information Criterion (BIC). Most significant improvement of the fit determined the inclusion of the variable. The process was repeated until no variable improved the model. The table shows the final remaining variables. The first variable to be chosen according to the BIC was the EDSS score at baseline. Second, the thalamic DVR at baseline was added, but after that, no variable could produce a model with a lower BIC value. The predefined variables considered in model building are detailed in the Methods section.

^a For DVR variables, the odds ratio is calculated as 0.1-unit increase due to the scale of the variables as explained in the Methods section.

observation was classified as a predicted later disability progression, and if probability of disability progression was below 50%, it was classified as disability progression not predicted. The receiver operating characteristic curve was also estimated along with the area under curve (AUC) value. All tests were 2 tailed, and a *p* value <0.05 was considered statistically significant for all analyses.

Standard Protocol Approvals, Registrations, and Patient Consents

This study was approved by the Ethics Committee of the Hospital District of Southwest Finland, and all participants provided written informed consent according to the Declaration of Helsinki.

Data Availability

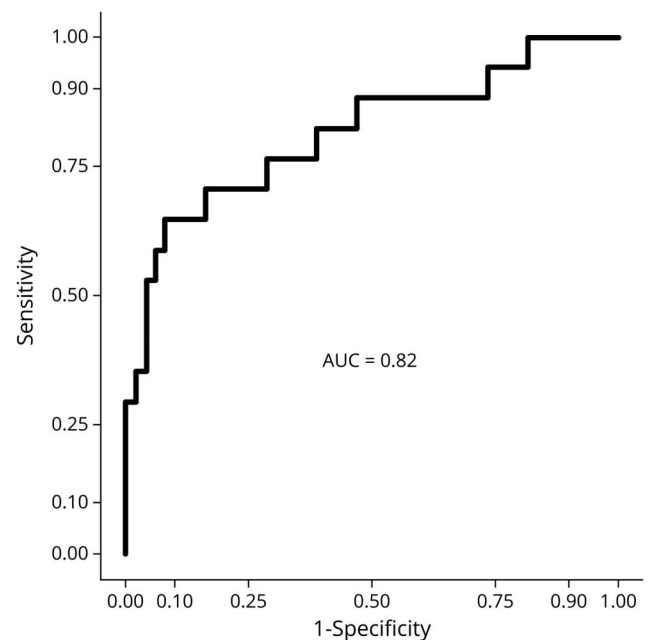
Anonymized data not published within the article will be shared over the next 3 years on request from a qualified investigator.

Results

Demographic and Clinical Characteristics of Participants

There were 47 patients with RRMS and 19 patients with SPMS in the final cohort. The mean age of the patients was 45.2 ± 9.9 years (mean ± SD), the mean disease duration at baseline was 12.4 ± 7.4 years, and the median EDSS score at baseline was 3.0 (interquartile range 2.0–3.9). The follow-up time for the final EDSS measurement was 3.0 ± 0.3 years (mean ± SD) after the initial evaluation. Altogether, 17 patients experienced disability progression during the follow-up, 6 of them patients with RRMS and 11 patients with SPMS. Altogether, 20 patients experienced a relapse during the follow-up. Of the 17 patients with demonstrable progression,

Figure 3 Receiver Operating Characteristic Curve From the Regression Model Using Leave-One-Out Cross Validation



The regression model predicted disability progression correctly in 9/17 patients (sensitivity = 52.9%) and no progression in 46/49 patients (specificity = 93.9%). The area under the curve (AUC) value for the model was 0.82.

only 7 experienced a relapse during follow-up. The demographic data and clinical variables of the cohort are shown in Table 1.

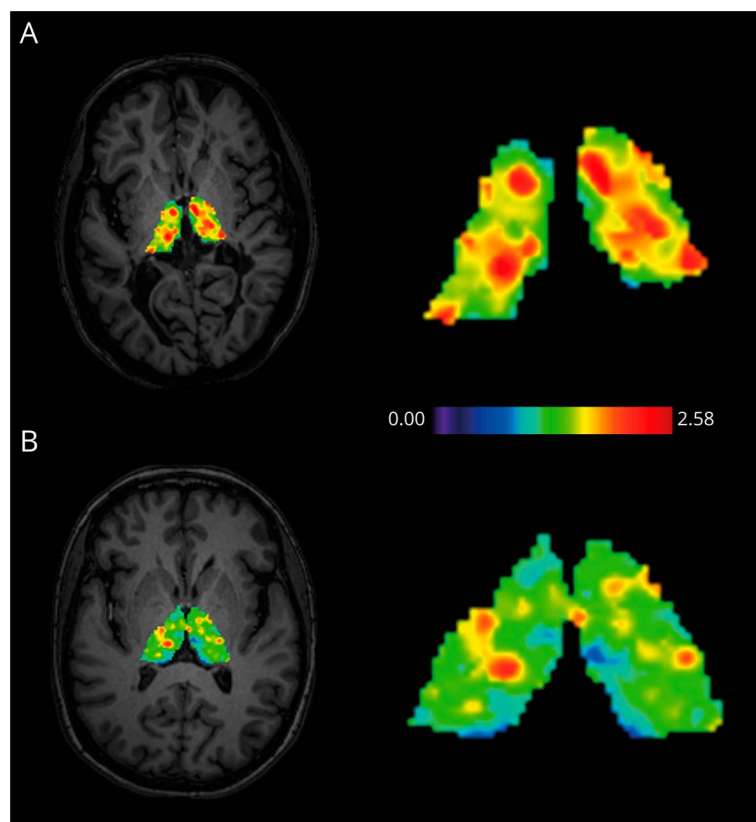
GM Innate Immune Cell-Related Pathology and Brain Volumetric Variables at Baseline

Patients with MS had a higher TSPO-PET DVR in the thalamus at baseline compared with healthy controls (mean ± SD 1.43 ± 0.10 vs 1.36 ± 0.06, *p* = 0.0066; Figure 1A). DVRs in the other deep GM ROIs did not significantly differ between patients with MS and healthy controls (Figure 1A). Likewise, the cortical GM DVR did not differ significantly between patients with MS and healthy controls (eFigure 1A, links.lww.com/NXI/A720). Patients with MS had lower PFs of the thalamus (0.0099 ± 0.0013 vs 0.0119 ± 0.0012, *p* < 0.001) and the caudate (0.0055 ± 0.0007 vs 0.0060 ± 0.0006, *p* = 0.014) at baseline compared with healthy controls (Figure 1B). Similarly, cortical GM PF of the patients (0.31 ± 0.03 vs 0.33 ± 0.02, *p* = 0.0017; eFigure 1B, links.lww.com/NXI/A720) differed from healthy controls at baseline. In the putamen and pallidum, no significant differences between patients with MS and healthy controls were observed (Figure 1B).

GM Innate Immune Cell-Related Pathology and Brain Volumetric Variables in Patients With and Without EDSS Progression

Patients with MS who experienced EDSS progression during the 3-year follow-up had a higher TSPO-PET DVR in the

Figure 4 Visualization of [^{11}C]-PK11195 Uptake Patterns in the Thalamus



(A) High thalamic DVR in a female patient with MS with disability progression during follow-up. The patient was 43 years old at baseline with a disease duration of 8.3 years. Her EDSS score was 6.5 at baseline and 7.0 at follow-up. (B) Low thalamic DVR in a female patient with MS without disability progression during follow-up. The patient was 52 years old at baseline with a disease duration of 9.0 years. Her EDSS score was 6.0 at baseline and 6.0 at follow-up. An axial T1W MRI slice is used to illustrate the anatomical position of the thalamus. The scale represents DVR values. DVR = distribution volume ratio; EDSS = Expanded Disability Status Scale.

thalamus compared with patients who did not progress (mean \pm SD 1.49 ± 0.10 vs 1.40 ± 0.09 , $p = 0.0028$; Figure 2A). The DVR in other ROIs did not associate with disability progression (Figure 2A and eFigure 1A, links.lww.com/NXI/A720). Regarding the MRI volumetric variables, the progressed patients had lower PFs of the thalamus (0.0092 ± 0.0015 vs 0.0102 ± 0.0011 , $p = 0.005$), caudate (0.0051 ± 0.0007 vs 0.0056 ± 0.0007 , $p = 0.04$), and putamen (0.0060 ± 0.0011 vs 0.0069 ± 0.0009 , $p = 0.002$) compared with patients who did not progress (Figure 2B). PFs of the pallidum (Figure 2B) and cortical GM (eFigure 1B, links.lww.com/NXI/A720) did not associate with disability progression.

Predictors of Disability Progression in the Regression Model

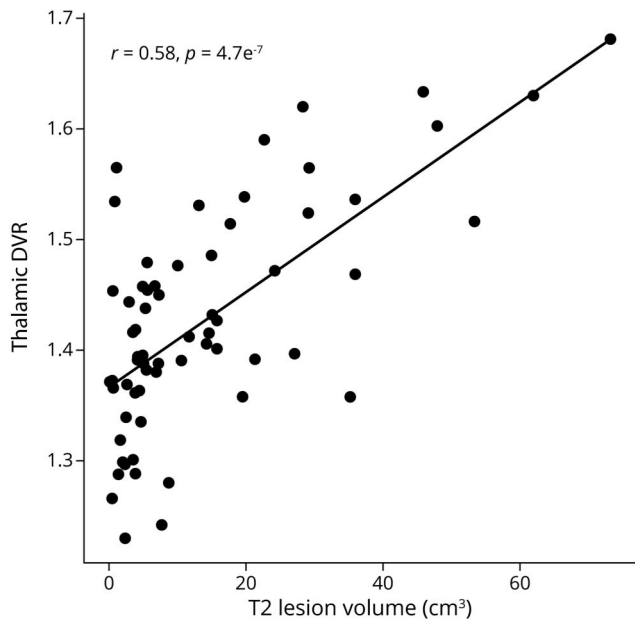
The EDSS score at baseline and thalamic TSPO-PET DVR at baseline remained significant predictors of disability progression in the forward-type stepwise logistic regression model (Table 2). No other imaging or clinical variable applied in the model improved the model further. A high EDSS score at baseline increased the odds of later disability progression (OR = 2.22; $p < 0.001$). Likewise, a high thalamic DVR at baseline increased the odds of progression (OR = 2.28; $p = 0.024$; OR calculated for 0.1 unit increase). The final regression model predicted disability progression with 52.9% sensitivity and 93.9% specificity with an AUC value of 0.82 (Figure 3). Figure 4 demonstrates a PET image from a patient

with a high thalamic DVR with later disability progression alongside a patient with a low thalamic DVR and no later disability progression. The thalamic TSPO-PET DVR correlated significantly with the global T2 lesion volume ($p < 0.001$; Figure 5). No statistically significant correlation was observed between the thalamic TSPO-PET DVR and cortical GM DVR or cortical GM volume (eFigure 2, links.lww.com/NXI/A720).

Discussion

This study provides evidence that thalamic innate immune cell-related pathology as measured using TSPO-PET predicts short-term disability progression in MS. The thalamic TSPO-PET DVR was the best imaging variable in the regression model to predict disability progression. High TSPO-PET signal in the MS thalamus has been demonstrated in several studies,^{11,12,15,17,24} and thalamic TSPO-PET signal has been linked with higher concomitant disability.¹⁷ The thalamic TSPO-PET signal reporting on increased innate immune cell-related pathology potentially reflects various ongoing disease mechanisms such as active focal inflammatory lesions in the thalamus or ongoing diffuse inflammation in the thalamus. It could also be a response to damage along distant WM tracts converging in thalamus or reflect inflammatory responses to neurodegeneration in the thalamus.¹ Thalamic

Figure 5 Association of Thalamic Innate Immune Cell Pathology With T2 Lesion Volume in the White Matter



High thalamic TSPO-PET DVR associated with high global T2 lesion volume. The Spearman correlation was used for statistical analysis. DVR = distribution volume ratio.

demyelinating lesions are a common finding in neuropathologic studies and are known to exhibit activated innate immune cells.^{25,26} Deep GM lesions appear to have intermediate inflammation compared with the abundant inflammation in the WM or the more scarce inflammatory findings in the cortical GM.^{25,27,28} Besides focal lesions, diffuse inflammation in the normal-appearing thalamus has been reported,²⁵ and of interest, lesional areas in the thalamus do not seem to have significantly higher TSPO-PET signal compared with the normal-appearing thalamus.¹⁷ Our MRI protocol did not allow for reliable identification of thalamic or other GM lesions, and we were unable to assess this aspect in our cohort.

A pathologic state of microglia and macrophages in the thalamus can be a response to damage along distant WM tracts converging in the thalamus.²⁹ Elevated thalamic TSPO-PET signal has been described in patients with ipsilateral cortical stroke linking innate immune cell activation with cortico-thalamic connection damage.³⁰ Likewise, facial nerve axotomy in rodents results in ipsilateral microglial activation in the facial nerve nucleus.³¹ In patients with MS, higher thalamic TSPO-PET signal has been associated with global cortical thinning,¹⁷ and decreased neuronal cell density can be seen histopathologically in individual thalamic nuclei in response to diffuse damage to the corresponding thalamocortical projections.³² Radiologically, thalamic atrophy and microstructural damage has been linked with global WM lesion load.^{33,34} A recent study has demonstrated that degeneration of efferent/afferent thalamic projections may in fact contribute more to thalamic atrophy than thalamic demyelinating

lesions.³⁵ Similarly, in traumatic brain injury, thalamic microglial activation has been observed in response to damage in distant WM areas.³⁶ In line with these findings, we report that the global T2 lesion volume increases as thalamic innate immune-cell related pathology increases. Global T2 lesion volume, however, did not survive as a significant predictor of disability progression in the regression model.

Compared with the thalamus, other deep GM regions in our cohort exhibited lower TSPO binding, and their activity was not associated with disability progression. The thalamus is a highly connected relay center of the brain³⁷ and may hence be more susceptible to Wallerian and transneuronal degeneration than the other deep GM structures. The thalamus is indeed known as a barometer for diffuse brain parenchymal damage in MS.³⁸

Thalamic atrophy has been extensively linked with disability and disease progression.³⁹⁻⁴¹ Similarly, atrophy in the other deep GM structures, including the caudate and putamen, has been associated with disease progression.^{5,7,42} In our cohort, atrophy in the thalamus, caudate, and putamen associated with disability progression in the first evaluations, but these parameters did not survive as significant predictors of disability progression in the regression model. This is likely linked to the fact that GM atrophy measures correlate strongly with the EDSS score⁶ and a high EDSS score predicts disability progression⁴³ as is also evident in our model. Once the EDSS score at baseline is added to the model, volumetric variables do not improve the model further. The thalamic DVR, on the other hand, remained in the model as an independent predictor, which suggests that thalamic innate immune cell-related pathology may be more sensitive than the atrophy measures to the thalamic disease processes that associate with short-term disability progression. Importantly, the thalamic DVR may predict progression in patients who have not yet entered the progressive disease trajectory indicated by atrophy and a high EDSS score. Inflammation in these patients could be therapeutically targeted to avoid later permanent neuroaxonal damage.

Studies addressing TSPO radioligand binding in the MS cortex have yielded variable results. Patients with MS have been shown to exhibit more cortical TSPO-PET signal than healthy controls, and this signal has been linked with higher disability.^{17,18} However, some work, including the present study, have failed to find differences in cortical TSPO-PET signal between patients with MS and controls.⁴⁴ This might reflect the lower signal-to-noise ratio of the first-generation TSPO radioligand [¹¹C]PK11195 compared with later-generation ligands.⁴⁵ On the other hand, the cortical TSPO-PET signal is highly prone to artifacts. The thin cortical GM is more abundantly vascularized than the WM⁴⁶ and anatomically close to the large meningeal blood vessels. As a consequence of this, the TSPO-PET signal obtained from the cortex may be significantly affected by both the endothelial

TSPO expression⁴⁷ and plasma protein bound radioligand within the bloodstream.⁴⁸

We have recently analyzed the effect of innate immune cell-related pathology in the NAWM regions of the MS brain to later disease progression.¹⁵ We demonstrated that innate immune cell-related pathology in periplaque regions predicted disability progression independent of relapses. This is in line with the concept that iron-containing innate immune cells at the edge of chronic active lesions promote lesion growth and disease progression.⁴⁹ In the present study, we focused on innate immune cell-related pathology in the GM regions of the MS brain. The main difference in the study design in the present work compared with the previously published study¹⁵ was the duration of the follow-up. The present cohort was more homogeneous in terms of the follow-up, with follow-up time ranging from 2.5 to 5.0 years with an average of 3.0 ± 0.3 years (mean \pm SD), whereas in our previous study, the follow-up time ranged between 2.0 and 9.5 years with an average of 4.1 ± 1.9 years (mean \pm SD).¹⁵ The time between the EDSS measurements was included as a covariate in the multiple linear regression model in both studies. It is plausible that the higher variability in the follow-up time in the previous study resulted with an alternative outcome regarding thalamic innate immune cell pathology and disease progression.¹⁵ Of interest, when we performed an additional analysis, where the NAWM DVR was included in the model, the thalamic DVR was still the strongest predictor of progression in the present cohort (data not shown). This implies that the thalamic DVR may be a better predictor for short-term progression compared with the NAWM DVR. It is noteworthy that it is more straightforward to radiologically identify the thalamic area in comparison to the perilesional areas of the smoldering lesions due to challenges in automated chronic WM lesion identification. Hence, measurement of neuroinflammation in the thalamus using TSPO-PET or potentially other, less technically demanding methods could be more easily incorporated into clinical practice, if TSPO-PET was to be used for evaluation of progression risk in a clinical setting in the future.⁵⁰

Our cohort included patients with both relapses and disability progression during the follow-up. The annual relapse rate during the follow-up was included in building the final model, but did not survive as an independent predictor of disability progression. This suggests that similarly to innate immune cell activation in periplaque white matter areas, thalamic innate immune cell activation associates more likely with diffuse neuroaxonal damage-promoting progression than with relapse-associated disease worsening. Unfortunately, the small number of patients with no relapses during the follow-up precluded us from formally testing the effect of the thalamic DVR on progression independent of relapses.

This study has some limitations. The sensitivity of the model is relatively low at 52.9%. This suggests that it might be

advisable to use additional complementary biomarkers to support thalamic TSPO-PET signal for more sensitive progression risk assessment. The population represents a real-world cohort and is heterogeneous in terms of DMTs. However, this was accounted for in the regression model. The brain MRI protocol was not optimal. We measured atrophy from a single MRI scan by using PFs. An atrophy rate calculated from several longitudinal scans could have captured the ongoing atrophy process more accurately. Finally, 2 different MRI scanners were used: a 3 T scanner for the majority of the population and an older 1.5 T scanner for a small subpopulation (10 patients with MS and 8 healthy controls). This may have induced noise in the data possibly impairing the performance of the volumetric variables. Importantly, the same PET camera was used throughout the study.

In conclusion, our study strengthens the concept of the innate immune cell-related pathology associating with gradual MS disease progression. Microglia and macrophages are versatile cells with a high range of phenotypes depending on the stage and nature of the ongoing CNS pathology.²⁹ Our work confirms that TSPO-PET-measurable innate immune cell-related pathology in the thalamus is an undesirable signal, reflecting a worse prognosis for patients with MS. This signal perhaps largely reflects both the diffuse and focal pathology affecting thalamic radiations as has been suggested for thalamic atrophy.³⁵ We hypothesize that thalamic innate immune cell-related pathology is an earlier and potentially modifiable signal of MS pathology (as opposed to thalamic atrophy) and, if detected, should be an indication for a therapeutic intervention. Future studies will show whether innate immune cell-targeting drugs will modify the status of these cells in the thalamus for the benefit of patients with MS.

Acknowledgment

All the study participants and the expert staff at Turku PET Centre are gratefully acknowledged for making this study possible.

Study Funding

Financial support for this study was provided by the Finnish Academy (decision number: 330902), the Sigrid Juselius Foundation, the state research funding of the Turku University Hospital expert responsibility area, and The Finnish MS Foundation and InFLAMES Flagship Programme of the Academy of Finland (decision number 337530).

Disclosure

The authors report no disclosures relevant to the manuscript. Go to [Neurology.org/NN](https://www.neurology.org/NN) for full disclosures.

Publication History

Received by *Neurology: Neuroimmunology & Neuroinflammation* December 7, 2021. Accepted in final form March 17, 2022. Submitted and externally peer reviewed. The handling editor was Friedemann Paul, MD.

Appendix Authors

Name	Location	Contribution
Olavi Misin, MD	Turku PET Centre, Turku University Hospital and University of Turku; Neurocenter, Turku University Hospital; Department of Clinical Neurosciences, University of Turku, Finland	Drafting/revision of the manuscript for content, including medical writing for content; major role in the acquisition of data; and analysis or interpretation of data
Markus Matilainen, PhD	Turku PET Centre, Turku University Hospital and University of Turku; Faculty of Science and Engineering, Åbo Akademi University, Turku, Finland	Analysis or interpretation of data
Marjo Nylund, MSc	Turku PET Centre, Turku University Hospital and University of Turku; Department of Clinical Neurosciences, University of Turku, Finland	Drafting/revision of the manuscript for content, including medical writing for content
Eveliina Honkonen, MSc	Turku PET Centre, Turku University Hospital and University of Turku, Finland	Drafting/revision of the manuscript for content, including medical writing for content
Eero Rissanen, MD, PhD	Turku PET Centre, Turku University Hospital and University of Turku, Turku, Finland	Major role in the acquisition of data
Marcus Sucksdorff, MD	Turku PET Centre, Turku University Hospital and University of Turku; Department of Clinical Neurosciences, University of Turku, Finland	Drafting/revision of the manuscript for content, including medical writing for content, and major role in the acquisition of data
Laura Airas, MD, PhD	Turku PET Centre, Turku University Hospital and University of Turku; Department of Clinical Neurosciences, University of Turku, Finland	Drafting/revision of the manuscript for content, including medical writing for content, and study concept or design

References

- Calabrese M, Magliozzi R, Ciccarelli O, Geurts JJ, Reynolds R, Martin R. Exploring the origins of grey matter damage in multiple sclerosis. *Nat Rev Neurosci*. 2015;16(3):147-158.
- Wattjes MP, Rovira À, Miller D, et al. Evidence-based guidelines: MAGNIMS consensus guidelines on the use of MRI in multiple sclerosis: establishing disease prognosis and monitoring patients. *Nat Rev Neurol*. 2015;11(10):597-606.
- Calabrese M, Romualdi C, Poretto V, et al. The changing clinical course of multiple sclerosis: a matter of gray matter. *Ann Neurol*. 2013;74(1):76-83.
- Eshaghi A, Prados F, Brownlee WJ, et al. Deep gray matter volume loss drives disability worsening in multiple sclerosis. *Ann Neurol*. 2018;83(2):210-222.
- Nourbakhsh B, Azevedo C, Maghzi AH, Spain R, Pelletier D, Waubant E. Subcortical grey matter volumes predict subsequent walking function in early multiple sclerosis. *J Neurol Sci*. 2016;366:229-233.
- Roosendaal SD, Bendfeldt K, Vrenken H, et al. Grey matter volume in a large cohort of MS patients: relation to MRI parameters and disability. *Mult Scler*. 2011;17(9):1098-1106.
- Jacobsen C, Hagemeyer J, Myhr KM, et al. Brain atrophy and disability progression in multiple sclerosis patients: a 10-year follow-up study. *J Neurol Neurosurg Psychiatry*. 2014;85(10):1109-1115.
- Popescu V, Klaver R, Voorn P, et al. What drives MRI-measured cortical atrophy in multiple sclerosis? *Mult Scler J*. 2015;21(10):1280-1290.
- Airas L, Rissanen E, Rinne J. Imaging neuroinflammation in multiple sclerosis using TSPO-PET. *Clin Transl Imaging*. 2015;3(6):461-473.
- Högel H, Rissanen E, Vuorimaa A, Airas L. Positron emission tomography imaging in evaluation of MS pathology in vivo. *Mult Scler*. 2018;24(11):1399-1412.

- Rissanen E, Tuisku J, Rokka J, et al. In vivo detection of diffuse inflammation in secondary progressive multiple sclerosis using PET imaging and the radioligand ¹¹C-PK11195. *J Nucl Med*. 2014;55(6):939-944.
- Sucksdorff M, Rissanen E, Tuisku J, et al. Evaluation of the effect of fingolimod treatment on microglial activation using serial PET imaging in multiple sclerosis. *J Nucl Med*. 2017;58(10):1646-1651.
- Debruyne JC, Versijpt J, Van Laere KJ, et al. PET visualization of microglia in multiple sclerosis patients using [¹¹C]PK11195. *Eur J Neurol*. 2003;10(3):257-264.
- Giannetti P, Politis M, Su P, et al. Increased PK11195-PET binding in normal-appearing white matter in clinically isolated syndrome. *Brain*. 2015;138(pt 1):110-119.
- Sucksdorff M, Matilainen M, Tuisku J, et al. Brain TSPO-PET predicts later disease progression independent of relapses in multiple sclerosis. *Brain*. 2020;143(3):3318-3330.
- Geurts JJ, Bö L, Pouwels PJ, Castelijns JA, Polman CH, Barkhof F. Cortical lesions in multiple sclerosis: combined postmortem MR imaging and histopathology. *AJNR Am J Neuroradiol*. 2005;26(3):572-577.
- Herranz E, Gianni C, Louapre C, et al. Neuroinflammatory component of gray matter pathology in multiple sclerosis. *Ann Neurol*. 2016;80(5):776-790.
- Politis M, Giannetti P, Su P, et al. Increased PK11195 PET binding in the cortex of patients with MS correlates with disability. *Neurology*. 2012;79(6):523-530.
- Schmidt P, Gaser C, Arsic M, et al. An automated tool for detection of FLAIR-hyperintense white-matter lesions in Multiple Sclerosis. *NeuroImage*. 2012;59(4):3774-3783.
- Rissanen E, Tuisku J, Vahlberg T, et al. Microglial activation, white matter tract damage, and disability in MS. *Neurol Neuroimmunol Neuroinflamm*. 2018;5(3):e443.
- Turkheimer FE, Edison P, Pavese N, et al. Reference and target region modeling of [¹¹C]-(R)-PK11195 brain studies. *J Nucl Med Official Publ Soc Nucl Med*. 2007;48(1):158-167.
- Yaqub M, Berckel BN, Schuitemaker A, et al. Optimization of supervised cluster analysis for extracting reference tissue input curves in (R)-[¹¹C]PK11195 brain PET studies. *J Cereb Blood Flow Metab*. 2012;32(8):1600-1608.
- Scolding N, Barnes D, Cader S, et al. Association of British Neurologists: revised (2015) guidelines for prescribing disease-modifying treatments in multiple sclerosis. *Pract Neurol*. 2015;15(4):273-279.
- Datta G, Colasanti A, Kalk N, et al. 11C-PBR28 and 18F-PBR111 detect white matter inflammatory heterogeneity in multiple sclerosis. *J Nucl Med*. 2017;58(9):1477-1482.
- Haider L, Simeonidou C, Steinberger G, et al. Multiple sclerosis deep grey matter: the relation between demyelination, neurodegeneration, inflammation and iron. *J Neurol Neurosurg Psychiatry*. 2014;85(12):1386-1395.
- Vercellino M, Maserà S, Lorenzatti M, et al. Demyelination, inflammation, and neurodegeneration in multiple sclerosis deep gray matter. *J Neuropathol Exp Neurol*. 2009;68(5):489-502.
- Mittelbronn M, Dietz K, Schluessener HJ, Meyermann R. Local distribution of microglia in the normal adult human central nervous system differs by up to one order of magnitude. *Acta Neuropathol*. 2001;101(3):249-255.
- Peterson JW, Bö L, Mörk S, Chang A, Trapp BD. Transected neurites, apoptotic neurons, and reduced inflammation in cortical multiple sclerosis lesions. *Ann Neurol*. 2001;50(3):389-400.
- Guerrero BL, Sicotte NL. Microglia in multiple sclerosis: friend or foe?. *Front Immunol*. 2020;11:374.
- Pappata S, Levasseur M, Gunn RN, et al. Thalamic microglial activation in ischemic stroke detected in vivo by PET and [¹¹C]PK11195. *Neurology*. 2000;55(7):1052-1054.
- Tay TL, Mai D, Dautzenberg J, et al. A new fate mapping system reveals context-dependent random or clonal expansion of microglia. *Nat Neurosci*. 2017;20(6):793-803.
- Kolasinski J, Stagg CJ, Chance SA, et al. A combined post-mortem magnetic resonance imaging and quantitative histological study of multiple sclerosis pathology. *Brain*. 2012;135(pt 10):2938-2951.
- Cappellani R, Bergsland N, Weinstock-Guttman B, et al. Subcortical deep gray matter pathology in patients with multiple sclerosis is associated with white matter lesion burden and atrophy but not with cortical atrophy: a diffusion tensor MRI study. *AJNR Am J Neuroradiol*. 2014;35(5):912-919.
- Louapre C, Govindarajan ST, Gianni C, et al. Heterogeneous pathological processes account for thalamic degeneration in multiple sclerosis: insights from 7 T imaging. *Mult Scler*. 2018;24(11):1433-1444.
- Mahajan KR, Nakamura K, Cohen JA, Trapp BD, Ontaneda D. Intrinsic and extrinsic mechanisms of thalamic pathology in multiple sclerosis. *Ann Neurol*. 2020;88(1):81-92.
- Scott G, Hellyer PJ, Ramlackhansingh AF, Brooks DJ, Matthews PM, Sharp DJ. Thalamic inflammation after brain trauma is associated with thalamo-cortical white matter damage. *J Neuroinflammation*. 2015;12(1):224.
- Herrero MT, Barcia C, Navarro JM. Functional anatomy of thalamus and basal ganglia. *Childs Nerv Syst*. 2002;18(8):386-404.
- Kipp M, Wagenknecht N, Beyer C, Samer S, Wuerfel J, Nikoubashman O. Thalamus pathology in multiple sclerosis: from biology to clinical application. *Cell Mol Life Sci*. 2015;72(6):1127-1147.
- Azevedo CJ, Cen SY, Khadka S, et al. Thalamic atrophy in multiple sclerosis: a magnetic resonance imaging marker of neurodegeneration throughout disease. *Ann Neurol*. 2018;83(2):223-234.
- Calabrese M, Rinaldi F, Mattisi I, et al. The predictive value of gray matter atrophy in clinically isolated syndromes. *Neurology*. 2011;77(3):257-263.
- Horakova D, Dwyer MG, Havrdova E, et al. Gray matter atrophy and disability progression in patients with early relapsing-remitting multiple sclerosis: a 5-year longitudinal study. *J Neurol Sci*. 2009;282(1-2):112-119.

42. Zivadinov R, Bergsland N, Dolezal O, et al. Evolution of cortical and thalamus atrophy and disability progression in early relapsing-remitting MS during 5 years. *AJNR Am J Neuroradiol*. 2013;34(10):1931-1939.
43. Fambias A, Jokubaitis V, Horakova D, et al. Risk of secondary progressive multiple sclerosis: a longitudinal study. *Mult Scler*. 2020;26(1):79-90.
44. Kaunzner UW, Kang Y, Monohan E, et al. Reduction of PK11195 uptake observed in multiple sclerosis lesions after natalizumab initiation. *Mult Scler Relat Disord*. 2017;15:27-33.
45. Ching AS, Kuhnast B, Damont A, Roeda D, Tavitian B, Dollé F. Current paradigm of the 18-kDa translocator protein (TSPO) as a molecular target for PET imaging in neuroinflammation and neurodegenerative diseases. *Insights Imaging*. 2012;3(1):111-119.
46. Hase Y, Ding R, Harrison G, et al. White matter capillaries in vascular and neurodegenerative dementias. *Acta Neuropathol Commun*. 2019;7(1):16.
47. Cosenza-Nashat M, Zhao ML, Suh HS, et al. Expression of the translocator protein of 18 kDa by microglia, macrophages and astrocytes based on immunohistochemical localization in abnormal human brain. *Neuropathol Appl Neurobiol*. 2009;35(3):306-328.
48. Chen MK, Guilarte TR. Translocator protein 18 kDa (TSPO): molecular sensor of brain injury and repair. *Pharmacol Ther*. 2008;118(1):1-17.
49. Hametner S, Dal Bianco A, Trattig S, Lassmann H. Iron related changes in MS lesions and their validity to characterize MS lesion types and dynamics with Ultra-high field magnetic resonance imaging. *Brain Pathol*. 2018;28(5):743-749.
50. Chiang GC, Hu J, Morris E, Wang Y, Gauthier SA. Quantitative susceptibility mapping of the thalamus: relationships with thalamic volume, total gray matter volume, and T2 lesion burden. *AJNR Am J Neuroradiol*. 2018;39(3):467-472.

Neurology[®] Neuroimmunology & Neuroinflammation

Innate Immune Cell–Related Pathology in the Thalamus Signals a Risk for Disability Progression in Multiple Sclerosis

Olavi Misin, Markus Matilainen, Marjo Nylund, et al.
Neurol Neuroimmunol Neuroinflamm 2022;9;
DOI 10.1212/NXI.0000000000001182

This information is current as of May 17, 2022

Updated Information & Services	including high resolution figures, can be found at: http://nn.neurology.org/content/9/4/e1182.full.html
References	This article cites 50 articles, 10 of which you can access for free at: http://nn.neurology.org/content/9/4/e1182.full.html##ref-list-1
Subspecialty Collections	This article, along with others on similar topics, appears in the following collection(s): Multiple sclerosis http://nn.neurology.org/cgi/collection/multiple_sclerosis PET http://nn.neurology.org/cgi/collection/pet
Permissions & Licensing	Information about reproducing this article in parts (figures,tables) or in its entirety can be found online at: http://nn.neurology.org/misc/about.xhtml#permissions
Reprints	Information about ordering reprints can be found online: http://nn.neurology.org/misc/addir.xhtml#reprintsus

Neurol Neuroimmunol Neuroinflamm is an official journal of the American Academy of Neurology. Published since April 2014, it is an open-access, online-only, continuous publication journal. Copyright Copyright © 2022 The Author(s). Published by Wolters Kluwer Health, Inc. on behalf of the American Academy of Neurology.. All rights reserved. Online ISSN: 2332-7812.

